Applied Microbiology and Biotechnology (2022) 106:8021–8034
https://doi.org/10.1007/s00253-022-12255-9

BIOTECHNOLOGICAL PRODUCTS AND PROCESS ENGINEERING

Chemical characterization and microencapsulation of extracellular fungal pigments

Paulina I. Contreras-Machuca[1,2] · Marcia Avello[1] · Edgar Pastene[3] · Ángela Machuca[4] · Mario Aranda[5] · Vicente Hernández[6,7] · Marcos Fernández[2]

Received: 11 July 2022 / Revised: 18 October 2022 / Accepted: 23 October 2022 / Published online: 12 November 2022

Abstract

In this work, extracellular colored metabolites obtained from the filamentous fungi *Talaromyces australis* and *Penicillium murcianum*, isolated in the Andean-Patagonian native forests of Chile, were studied as prospect compounds to increase the sustainability of cosmetic products. The chemical and antioxidant properties of these natural pigments were characterized and strategies for their microencapsulation were also studied. UHPLC/MS–MS analyses indicated that the predominant metabolites detected in the cultures of *P. murcianum* were monascin ($m/z = 411.15$) and monashexenone ($m/z = 319.10$), while athrorosin H ($m/z = 458.20$) and damnacanthal ($m/z = 281.05$) were detected in cultures of *T. australis*. ORAC tests revealed that *P. murcianum*'s metabolites had the greatest antioxidant properties with values higher than 2000 µmol of trolox equivalents/g. The fungal metabolites were successfully microencapsulated by ionic gelation into structures made of 1.3% sodium alginate, 0.2% chitosan, and 0.07% hyaluronic acid. The microencapsulation process generated structures of 543.57 ± 0.13 µm of mean diameter (d_{50}) with an efficiency of 30% for *P. murcianum*, and 329.59 ± 0.15 µm of mean diameter (d_{50}) and 40% efficiency, for *T. australis*. The chemical and biological characterization show the biotechnological potential of these fungal species to obtain pigments with antioxidant activity that could be useful in the cosmetic industry. The encapsulation process enables the production of easy-to-handle dry powder from the fungal metabolites, which could be potentially marketed as a functional cosmetic ingredient.

Key points

- *The predominant fungal pigments were of azaphilone and anthraquinoid classes.*
- *The fungal pigments showed high antioxidant activity by ORAC assay.*
- *Fungal pigment microcapsules obtained by ionic gelation were characterized.*

Keywords Fungal pigments · Azaphilones · Anthraquinoids · Mass spectrometry · ORAC assay · Ionic gelation

Introduction

Today, the society exerts greater pressure on products manufactured from novel raw materials, with a reduced content of additives and synthetic chemicals that can increase toxicity. This is due to the different risks that can be presented either during the research and development of new products, or in its impact once it is distributed in the population. In this way, greater environmental regulations have been implemented in some countries, where the use of many synthetic chemical compounds has been limited or prohibited, encouraging the search of new molecules and technologies that are more environmentally friendly and safe for those who manipulate or use them (Chemat et al. 2012). For this reason, there is a great interest in natural products derived from microorganisms, since they have the advantage that can be easily cultivated and optimized for the production of certain metabolites such as pigments (Patil et al. 2016; Li et al. 2018). Natural pigments have traditionally been obtained from plants, but various problems related with their production have led to the search for alternative sources such as fungi (Caro et al. 2015). Fungal pigments, unlike plant pigments, have the advantage of being mainly extracellular metabolites

✉ Paulina I. Contreras-Machuca
paucontrerasm@udec.cl; paucontrerasm@hotmail.com

✉ Ángela Machuca
angmachu@udec.cl

Extended author information available on the last page of the article

and therefore the recovery from the culture broths is a relatively simple process (Sajid and Akbar 2018). In addition, the fungal pigments can be produced under laboratory conditions, in confined spaces, regardless of seasonality (Galindo et al. 2007). Due to this, several filamentous fungi belonging to the genera *Monascus*, *Fusarium*, *Penicillium*, and *Talaromyces*, among others, are being investigated as important sources of natural pigments (Feng et al. 2012; Morales et al. 2020; Pitt and Hocking 2022). Among that, *Monascus* pigments have been used by humans since ancient times, and therefore, these pigments are among the most extensively investigated and described in the literature (Gao et al. 2013; Gmoser et al. 2017; Chaudhary et al. 2022).

To date, a large number of polyketide compounds have been described in fungi, of which an interesting group with multiple beneficial properties corresponds to pigments of the azaphilone type (Feng et al. 2012; Pimenta et al. 2021). The *Monascus* yellow pigment azaphilone type, monascin, has been related to the reduction of oxidative stress in animal models, activating enzymes and transcription factors involving in metabolism, resistance to stress, and antioxidant reserves (Shi and Pan 2012). Another group of polyketide pigments that are present in species of filamentous fungi of the genera *Penicillium*, *Talaromyces*, and *Aspergillus* are the hydroxyanthraquinoids, which also shows important antioxidant and antimicrobial activities (Caro et al. 2012; Li et al. 2017). For these reasons, antioxidant fungal pigments show a great potential in the formulation of dyes safer than synthetic dyes of traditional use such as azo, triphenylmethane, and xantene derivatives, widely used in the cosmetic industry, but having a history of cytotoxicity (Crebelli et al. 1981; Combes and Haveland-Smith 1982). In accordance with the above, it is necessary to increase the search and characterization of new fungal pigments with biological properties of interest and potential use in the cosmetic industry (Pimenta et al. 2021). *Penicillium* and *Talaromyces* species are promising because they are neither mycotoxigenic nor pathogenic for humans, and on the contrary, they can present beneficial characteristics for health. These include antioxidant, antimicrobial, and anti-inflammatory properties (Gao et al. 2013; Gmoser et al. 2017; Morales et al. 2020; Poorniammal et al. 2021). Pigments obtained from *Talaromyces* and *Penicillium* species are generally considered of low toxicity. However, the successful application of these metabolites as new functional ingredient depends on their correct characterization and the results of toxicity studies performed in accordance with EU and FDA regulations (Morales et al. 2020; Poorniammal et al. 2021). In specific, toxicity studies with pigments from these fungi revealed a low toxicity and their suitability to be used in textile applications (Hernández et al. 2019). *P. murcianum* and *T. australis*, isolated from decay wood in forest of central-south Chile, have demonstrated to be efficient pigment producers. The pigments from these two fungal species have already been used in the dyeing of fabrics for textile purposes (Hernández et al. 2018a,b, 2019, 2020), but they have not yet been chemically characterized.

The stabilization of natural pigments for their posterior incorporation into cosmetic formulation can be achieved by microencapsulation. This process grants protection and special properties to the encapsulated product. For instances, encapsulation can provide protection against adverse environments, stabilize sensitive drugs, and generate a controlled or prolonged release system. Microencapsulation can be used to protect natural pigments from oxidative processes, light, humidity, etc., maintaining a more intense and prolonged coloration (Swarbrick 2006; Jurić et al. 2020).

The main objective of the present study was to characterize the extracellular colored pigments produced by the filamentous fungi *Penicillium murcianum* and *Talaromyces australis*, evaluating their biological activity through antioxidant capacity, and determining the viability of its microencapsulation. Studies on the chemical nature of these fungal pigments are necessary in order to support their use in new application, in areas such as the cosmetic industry (Pimenta et al. 2021).

Material and method

Fungal strains and liquid cultures for pigment production

The filamentous fungi *Penicillium murcianum* PM 2015 and *Talaromyces australis* TA 2015 were isolated of decayed wood samples collected in central Chile. The fungi were identified through molecular techniques, by sequencing of the ribosomal DNA ITS region (Hernández et al. 2018b), and deposited under code RGM 2467 (*P. murcianum*) and RGM 2468 (*T. australis*) in the Chilean Collection of Microbial Genetic Resources (CChRGM) at the Instituto de Investigaciones Agropecuarias (INIA, Chile). This entity is associated to the World Data Centre for Microorganisms (WDCM) under the accession acronym CChRGM and number WDCM 1067. These fungi were grown in flasks containing 500 mL of optimized nutrient medium, peptone-glucose-yeast extract (PGY), adjusted at pH 5 for *T. australis* and pH 9 for *P. murcianum* (Hernández et al. 2019). The PGY medium consisted of 12 g/L glucose and 0.1 g/L yeast extract for both fungi, with different peptone concentrations, 11 g/L for *T. australis* and 20 g/L for *P. murcianum*. In addition, the medium for *P. murcianum* was supplemented with NaCl (6 g/L). After a 20-day incubation period, at 28 °C under agitation (120 rpm), the cell-free extracts were obtain after paper filtration. The filtered extracts containing extracellular pigments of each species were then frozen at − 18 °C and kept in these conditions until use.

Crude extracts

Initially, a glass column (60 × 10 cm) filled with Amberlite XAD-16 resin (Sigma-Aldrich) was used in order to separate the extracellular fungal pigments from salts and compounds highly soluble in water. For that, 100 mL of each filtered extract was added to the column and once the color was absorbed by the resin, it was washed several times with distilled water until the supernatant became transparent. Then, the adsorbed pigments were eluted from the column with methanol and the collected fractions were concentrated in a Heidolph (Schwabach, Germany) rotary evaporator Laborota 4000/4001 efficient, getting a yellow-brown crude extract for *P. murcianum* and a red-yellow crude extract for *T. australis*. The yield of the crude extracts was expressed as milligram of extract per milliliter of filtered broth.

Separation by centrifugal partition chromatography (CPC)

Crude extracts were fractionated using the CPC instrument Armen (Armen, France) Spot-CPC 250-L centrifugal partition chromatograph with a 250 mL total cell volume and a four-way switching valve that allows operation in either the descending or ascending modes (Ying et al. 2014). The CPC system was connected to a SPOT-PREP-II system, with integrated UV detector and fraction collector, and Armen Glider software package. The separation by CPC was performed in descending mode with a two-phase solvent systems composed of ethyl acetate/butanol/water 1:1:2 (v/v/v) for *P. murcianum* and 4:1:5 (v/v/v) for *T. australis*. In the second case, another solvent system with butanol/water 1:1 (v/v) was developed to improve the separation of the most polar pigments. The solvent mixture was automatically generated by the SPOT-PREP-II unit. The CPC rotor was first filled with organic phase at 30 mL/min and 500 rpm rotation. Lower phase was pumped into the system in the descending mode at a flow rate of 24 mL/min and rotation was increased from 0 to 2200 rpm for *P. murcianum* and 1800 rpm para *T. australis*. After equilibrium was reached, the samples were dissolved in 10 mL 1:1 mixture of upper and lower layers and injected into the CPC system (10 mL sample loop). Elution was monitored using scan 280, 350, 430, and 510 nm wavelengths, collecting 45 fractions in 20 mL tubes (Figure S1). Fractions were analyzed by HPLC and those with similar composition were combined in fractions according with their online UV–Vis spectra obtained from the preparative detector. The samples that presented the highest amount of pure pigment were selected from the chromatographic analysis.

Analysis of fractions by ultra-high-performance liquid chromatography (UHPLC) with a diode array detector (DAD) and tandem mass spectrometry (MS and MS–MS)

Chromatography was performed in Shimadzu (Kyoto, Japan) Nexera X2 UHPLC system composed of LC-30 AD pump, DGU-20A5R degassing unit, SIL-30 AC autosampler, CTO-20 AC column oven, CBM-20A communication module, SPM-M20A diode array detector (DAD), and LCMS-8030 triple quadrupole (TQ) mass spectrometer (MS) equipped with an electrospray ionization source (ESI). MS analysis was performed using the following settings: ESI (−) voltage of 4.5 kV; nebulizer gas (N_2) flow: 3.0 L/min; drying gas (N_2) flow: 15 L/min; desolvation line (DL) temperature: 250 °C; and heat block temperature: 400 °C. Data were acquired, recorded, and analyzed by means of the Shimadzu LabSolution 5.8 software. The methodology was developed as described for *Monascus*-type pigments with modifications (Inoue et al. 2010). A Kromasil 100-5-Phenyl column of 4.6 × 250 mm, particle size 5 µm, series M05PHA25/E164679, at 40 °C was used. The injection volume was 20 µL for all samples. A mobile phase gradient was established, consisting of 0.2% formic acid in water (solvent A) and 0.2% formic acid in methanol (solvent B). In this case, it was started at 0 min, 55% of solvent B, gradually increasing it to 90% at 15 min and during the following minutes, the gradient was balanced until reaching the proportions of the initial phase system at 30 min. Assays were performed with a flow rate of 0.6 mL/min. The analysis was performed with electrospray ionization (ESI) in negative polarity and two types of analysis were performed: scan mode (SM), in this case the mass values recorded were 50–2000 mass–charge ratio (*m*/*z*), and product ion scan (PIS), where the fractional *m*/*z* were selected, which corresponded to the values of the main pigments.

Evaluation of antioxidant capacity through assays of oxygen radical absorption capacity tests (ORAC)

Crude extracts and purified fractions of both fungal species were evaluated by monitoring the fluorescence decay in a fluorescein target oxidized by the 2,2′-azobis (2-methylpropionamidine) dihydrochloride (AAPH) radical, in a Fluorescence Spectrometer Perkin Elmer (Waltham, MA, USA). The ORAC-FL assay was performed according with literature (Ou et al. 2013), with some modifications. In a 96-well black plate, 150 µL of 0.11 µM fluorescein was added to each well. Then, 25 µL phosphate buffer (blank) and Trolox® (standard curve between 25 and 50 µM) were added to each well. The assay was placed to incubate for 30 min at 37 °C. Then, 25 µL AAPH was quickly added to each well and measurements were taken up between 0

and 120 min, measuring every 1 min, with an excitation and emission wavelength of 485 and 539 nm, respectively at 37 °C. A calibration curve was obtained through the equation of a linear regression of the area under the fluorescein decrease curve (AUC), versus the Trolox® concentration. ORAC values for the samples were obtained using the calibration curve and expressed as µmoles of Trolox® equivalents (TE) per gram of sample (µmol TE/g).

Microencapsulation of fungal pigments by vibration nozzle

Hybrid microcapsules were made by ionic gelation following the instructions provided on the operating manual of the B-390 BÜCHI microencapsulator (Flawil, Switzerland) (BÜCHI Labortechnik AG 2016) and literature (Yan et al. 2015; Athamneh et al. 2019), with some modifications. For this, *T. australis* and *P. murcianum* crude extracts (treated with Amberlite XAD-16) were added separately in a mixture of 1.3% w/v sodium alginate and 0.07% w/v hyaluronic acid (95/5) to a final volume of 100 mL. For *P. murcianum*, the parameters of the process used on the microencapsulation were fixed as follows: vibrational frequency of the membrane: 400 Hz; electrode potential: 2000 V; air pressure: 229 mbar; flow: 15 mL/min; nozzle temperature: 40 °C; and nozzle diameter: 450 µm. For *T. australis*, the parameters were as follows: vibrational frequency of the membrane: 700 Hz; electrode potential: 2300 V; air pressure: 462 mbar; flow: 8 mL/min; nozzle temperature: 40 °C; and nozzle diameter: 300 µm. The microdroplets expelled from the equipment were received in an ionic bath containing a mixture of 0.2 M calcium chloride and 0.2% w/v chitosan (3/1) under constant stirring. The obtained microcapsules were then vacuum filtered through a 10-µm membrane filter, washed with 200 mL of nanopure water, frozen at − 20 °C, and finally dried in a Xiang Yi LGJ-10C (China) lyophilizer for 24 h.

Color of fungal pigment microcapsules

The color of the fungal pigments microcapsules was measured on a CM-5 Konica Minolta (NJ, USA) spectrophotometer. For the measurements, a 0.60 g sample was taken from each type of fungal microcapsule and deposited on different transparent plastic plates. Reflectance reading on the spectrophotometer were then carried out, registering the color on the CIE L^* a^* b^* coordinates, where L^* corresponds to lightness from 0 (black) to 100 (white), a^* from − 60 to + 60 (greenness-blueness), and b^* from –60 to + 60 (blueness-yellowness) (Mapari et al. 2006). In addition, from the coordinates, the values c^* (saturation) and h^* (hue) were also obtained (Ohta and Robertson 2005).

Granulometric analysis by optical and scanning electron microscopy

In order to evaluate the microencapsulation process, fungal pigment microcapsules were first observed under a Primo Star Zeiss (Germany) optical microscope, with a 4× magnification. Later on, a Tescan Vega 3 SBU Easyprobe (Kohoutovice, Czech Republic) scanning electron microscope (SEM) was used to analyze the microcapsules. SEM was performed at the Center for Advanced Microscopy, CMA Bio-Bio, Concepción, Chile.

Morphology of microcapsules was defined according to the classification described in United States Pharmacopeia No. 30 (USP 30) (Convention 2007b) for light microscopy. For size distribution determination, the Feret diameter technique described in USP 30 (Convention 2007a) was used. This corresponds to the distance between imaginary parallel lines tangent to a randomly oriented particle perpendicular to the eyepiece scale. Observations were made on samples of 300 microcapsules per batch. Data were processed to obtain a frequency distribution table ordered by class intervals, in order to obtain the geometric and statistical mean diameters (Aulton 2002; Montenegro et al. 2011). Size distribution of the microcapsules was described quantitatively using the particle size dispersal coefficient (Span) calculated according to $\text{Span} = (d_{90} - d_{10})/d_{50}$, where d_n ($n = 10$, 50, and 90) denotes the particle diameter at 10%, 50%, and 90% of the size distribution. A low Span is indicative of a more homogeneous size distribution (Xiao et al. 2005).

Determination of encapsulation efficiency by spectrophotometry

Determination of encapsulation efficiency was performed according to the methodology established by Aizpurua-Olaizola et al. (2016) with modifications. A mass of microcapsules was ground as finely as possible with a mortar. From this, 3 samples were taken for each of the species and 7.5 mL of 0.3 M sodium citrate was added to each of them. Then, the mixtures were subjected to high-frequency stirring with a digital Ultra Turrax® IKA T18, gradually increasing the frequency up to 21,000 rpm, in order to obtain a homogeneous mixture. The mixtures were then incubated in an ELMA Transsonic 820 / H ultrasound bath for 2 h. Once this process was finished, 15 mL of methanol was added to precipitate the polymer and obtain an extract of the pigments. Pigment extracts were evaluated by UV–Vis spectrophotometry in a Cary 50 conc Varian spectrophotometer (Pittsburgh, USA) at 400 nm for *P. murcianum* and 490 nm for *T. australis*. The absorbance measurements correspond to the amount of encapsulated pigment.

Statistical analysis

Data were evaluated using descriptive statistics using the Minitab 19 software (Pennsylvania, USA) (mean, standard deviation (SD), and relative standard deviation (RSD)). Calibrations were established applying a linear regression model. Comparison of area under curve was done using the GraphPad Prism 6.01 software (San Diego, CA, USA).

Results

Crude extract yields

The culture broths, rich in pigments from both fungi (Fig. 1) and produced under optimized conditions (Hernández et al. 2019), were treated with Amberlite XAD-16 resin and then concentrated. The broths yielded 3 mg/mL of yellow and brown pigments in the case of *P. murcianum* and 5 mg/mL of mixture of red and yellow pigments for *T. australis*.

Separation of fungal extracts by CPC

After subjecting the crude extracts to liquid–liquid extraction with different biphasic solvent systems, the distribution of pigments between the phases of the same system was evaluated and the system that showed the best distribution of pigments was selected. Thus, the system ethyl acetate/butanol/water was selected for *P. murcianum* (1:1:2 v/v/v) and for *T. australis* (4:1:5 v/v/v). In a second test, a butanol/water system (1:1 v/v) was used for *T. australis*, achieving a better separation of pigments. Retention of the stationary phase corresponded to > 80%. After CPC, more than 35 fractions (20 mL) were obtained from the crude extracts of both fungi, separated in decreasing order of polarity (Figure S1).

Chemical characterization of *P. murcianum* samples

The chromatographic analysis generated fractions relatively pure of *P. murcianum* extracts. Multiple yellow compounds were detected whose mass–charge ratio values coincided with the molecular weight of several already known natural pigments. Most of them correspond to polyketides, such as azaphilones (Gao et al. 2013). Two samples, selected due to their purity and yield at CPC-HPLC, were selected for a product ion scan analysis. In the first sample (*P. murcianum* sample 1), the main signal of the chromatogram, at 446 nm and at retention time of 7.62 min (Fig. 2A), indicated the presence of compounds that absorb in the visible region. The spectrum registered in the range of 200–600 nm showed absorbance peaks mainly in the UV–Vis region. In the near UV–Vis region, there were peak values at 310, 371, 398, and 446 nm (Fig. 2B), which are characteristics for yellow pigments. Measurements in ESI–MS scan mode reveal values that could correspond to molecular ions of most pigments in the sample, where at least three mass values (*m*/*z*) of 411.15, 421.15, and 438.10 were observed (Fig. 2C). The MS–MS spectrum of the ion 421.15 describes at least 6 mass values, 144.30, 212.00, 240.90, 245.00, 255.00, and 257.20, that could correspond to the fragments formed (Fig. 2D) (Figure S2). In the second sample (*P. murcianum* sample 2), the signal of the main pigment obtained from the chromatogram

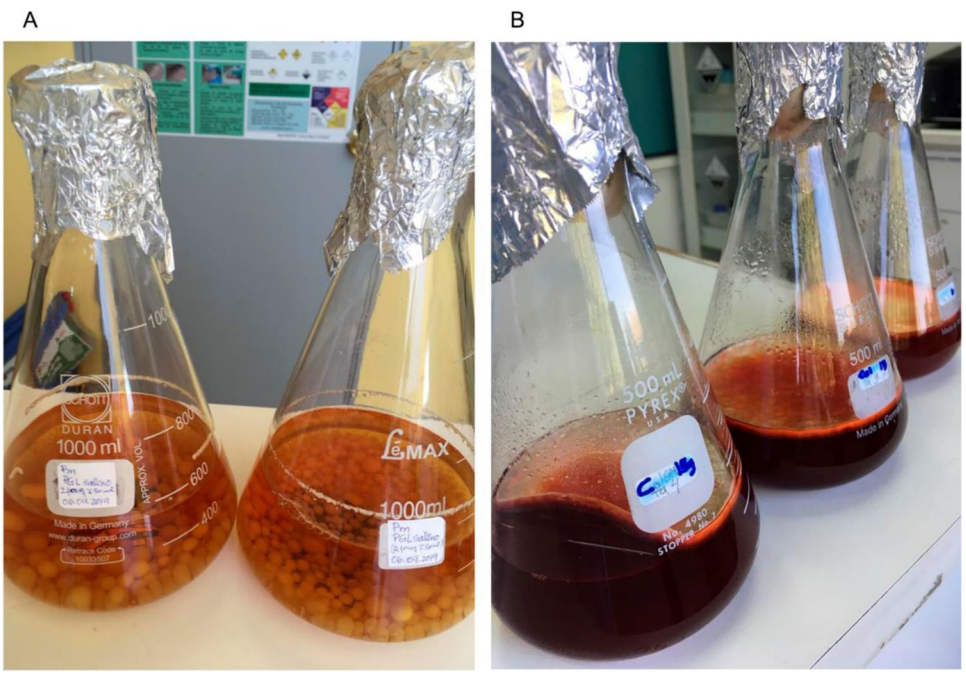

Fig. 1 Culture broths of the filamentous fungi *P. murcianum* (**A**) and *T. australis* (**B**) grown in PGY medium, under optimized conditions for production of extracellular red and yellow pigments, respectively

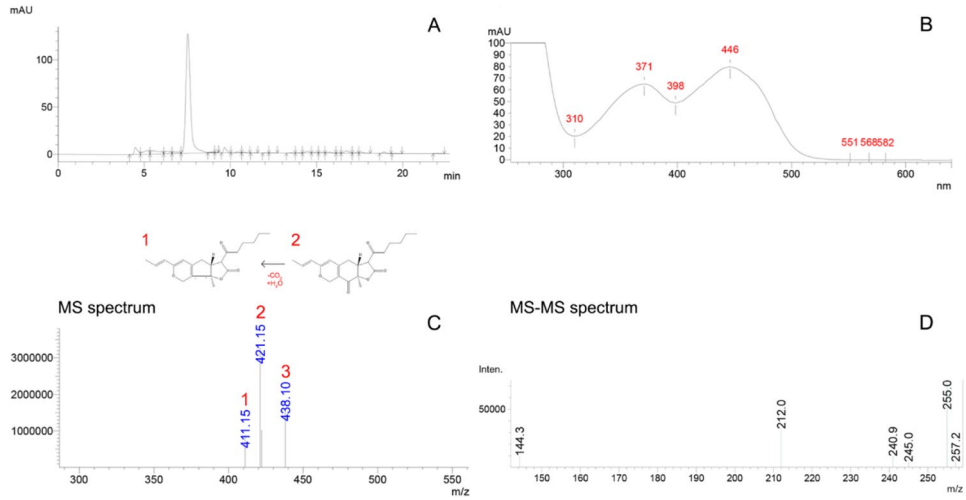

Fig. 2 **A** UHPLC chromatogram (t_R = 7.62 min). **B** Spectrogram of 200–600 nm. **C** Mass spectrum and chemical structure of monascin (numbering detail: 1 = [M-H-CO_2 + HCOOH + H_2O]$^-$, 2 = [M-H + HCOOH + H_2O]$^-$, 3 = [M-2H + HCOOH + 2H_2O].$^-$). **D** MS–MS spectrum from *P. murcianum* sample 1

at 430 nm shows a maximum at 12.00 min (Fig. 3A). Spectrograms in a range of 200–800 nm showed a peak in the far UV region. To a lesser extent, there were absorption peaks in the medium UV region at 278 and 312 nm. Finally, in the visible region, a notorious maximum of 407 nm, characteristic for yellow pigments, was observed (Fig. 3B). UHPLC-MS scan mode measurements showed a spectra with mass values of 319.10 (Fig. 3C). In the MS–MS spectrum of the main molecular ion, it was 319.10, and at least 14 mass values were obtained 83.30, 93.10, 95.00, 98.00,

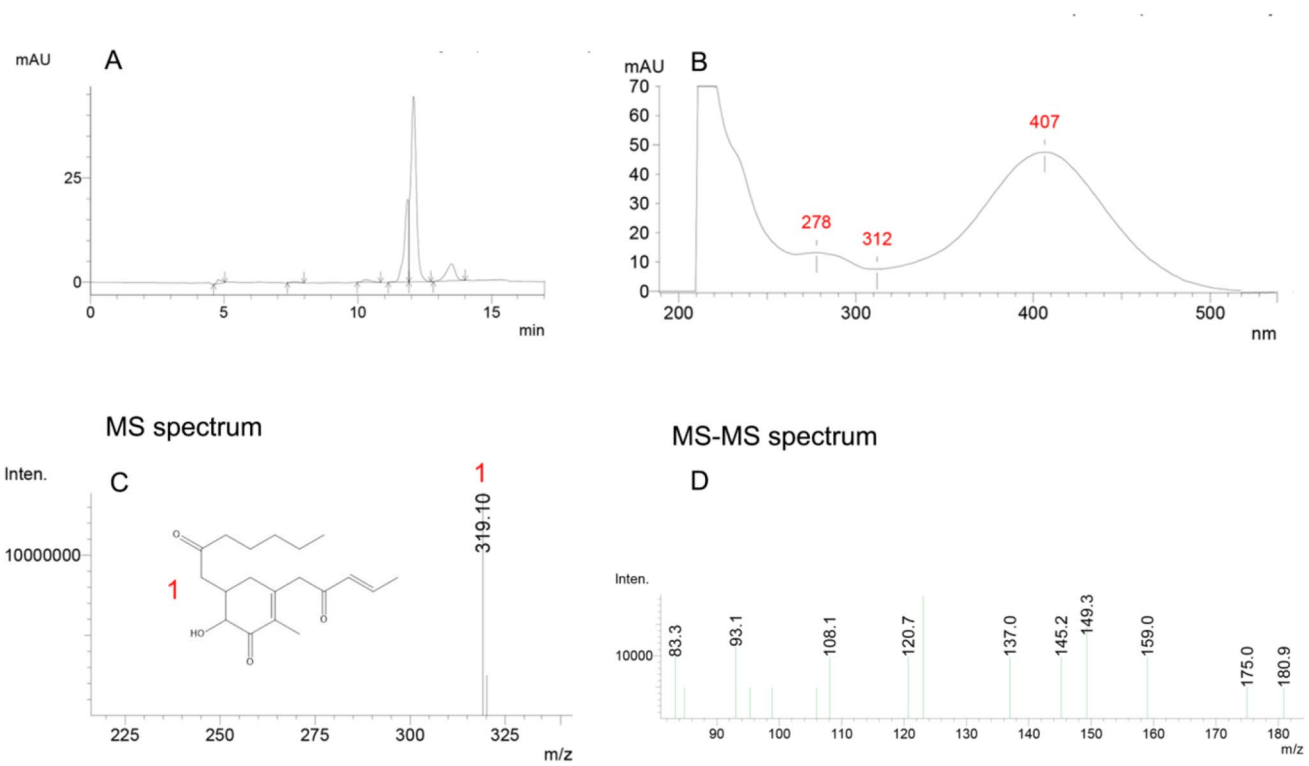

Fig. 3 **A** UHPLC chromatogram (t_R = 12.00 min). **B** UV–VIS spectrogram from 200 to 800 nm. **C** Mass spectrum and chemical structure of monashexenone (numbering detail: 1 = [M-H].$^-$). **D** MS–MS spectrum from *P. murcianum* sample 2

106.00, 108.10, 120.70, 123.00, 137.00, 145.20, 149.30, 159.00, 175.00, and 180.90 (Fig. 3D) (Figure S3).

Chemical characterization of *T. australis* samples

The chromatographic analysis of *T. australis* extracts showed the presence of less pure fractions since multiples peaks with low resolution were observed. This evidenced the complexity of the chemical composition of the extracts of this fungal specie. Two pigment fractions were analyzed; in the first one (*T. australis* sample 1), a chromatogram with low resolution among the numerous signals was obtained. The most notable was at 14.38 min (Fig. 4A). The spectrum showed peak values at 429, 458, and 505 nm (Fig. 4B), which are characteristics for yellow, orange, and red pigments. UHPLC-MS scan mode measurements indicate a spectrum with mass values of 548.20 (Fig. 4C). When analyzing the fragments obtained in the MS–MS spectrum, it was observed that for $[M\text{-}H]^- = 548.20$, at least 9 mass values were produced 167.00, 322.10, 338.90, 365.00, 408.90, 463.80, and 479.40 (Fig. 4D) (Figure S4). In the second sample (*T. australis* sample 2), the chromatogram showed a main signal at 9.95 min and 430 nm (Fig. 5A). Likewise, the UV–Vis spectrograms showed peak in the UV region. In the near UV region, there was a low signal at 312 nm and in the visible region, a peak at 405 nm was observed, which is characteristic for yellow pigments (Fig. 5B). The ESI–MS scan mode revealed a mass spectrum with the *m/z* value of 281.05 (Fig. 5C). When analyzing the fragments obtained in the MS–MS spectrum, it was observed that for the *m/z* value of 281.05, 14 mass values were produced 138.70, 150.50, 164.70, 170.10, 179.80, 183.00, 185.10, 194.00, 196.90, 207.60, 211.00, 212.90, 236.00, and 237.00 (Fig. 5D) (Figure S5).

Evaluation of antioxidant capacity through ORAC assay

Antioxidant activity tests were carried out with total extracts and with selected fractions based on the yield of the separation. In all cases, the antioxidant activity was positive, obtaining ORAC values of 118.2 µmol TE/g, 2130.40 µmol TE/g, and 477.50 µmol TE/g for *P. murcianum* total extracts, samples 1 and 2, respectively, and 239.2 µmol TE/g, 235.72 µmol TE/g, and 706.36 µmol TE/g for *T. australis* total extracts, samples 1 and 2, respectively. The major antioxidant activity over time for fractions is shown in Figure S6. Samples containing the complete fungal pigment

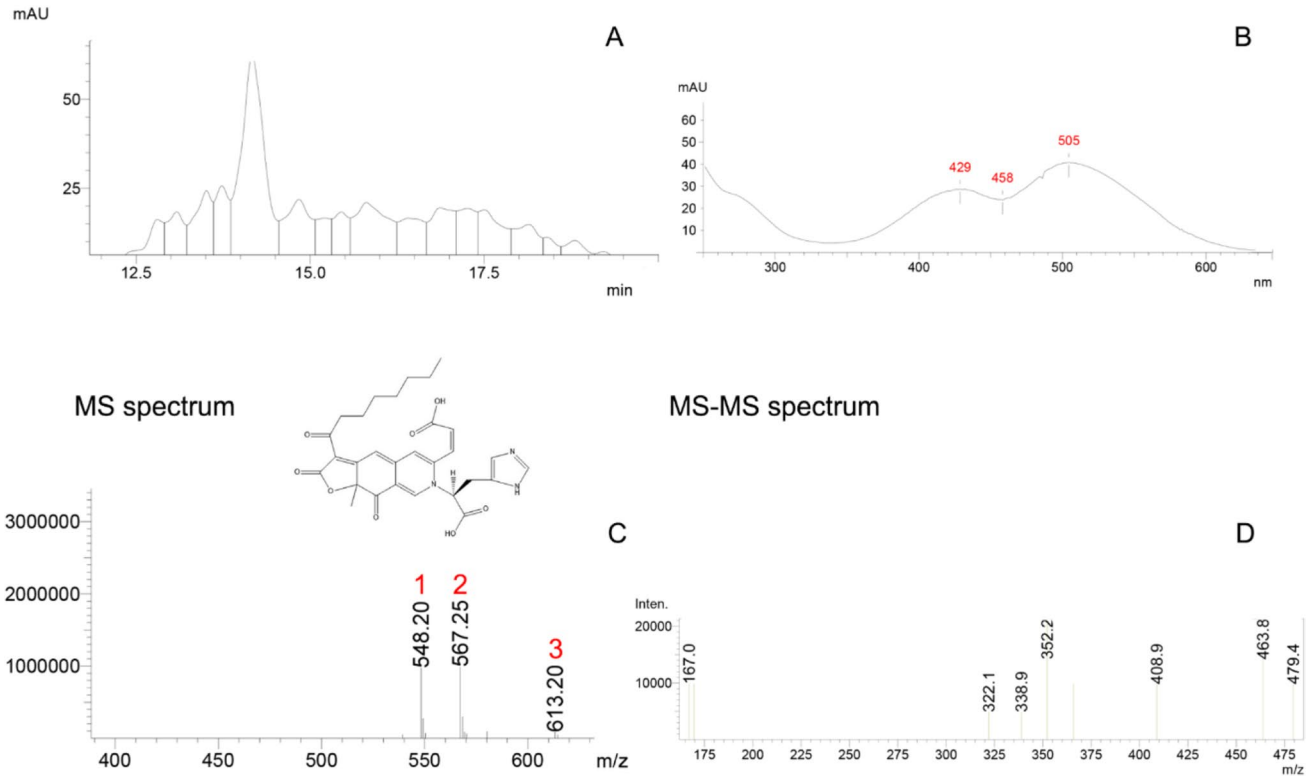

Fig. 4 **A** Chromatogram obtained by UHPLC ($t_R = 14.38$ min). **B** UV–VIS spectrogram from 200 to 800 nm. **C** Mass spectrum and chemical structure for atrorosin H (numbering detail: $1 = [M\text{-}H]^-$, $2 = [M + H_2O]^-$, $3 = [M + HCOOH + H_2O].^-$). **D** MS–MS spectrum from *T. australis* sample 1

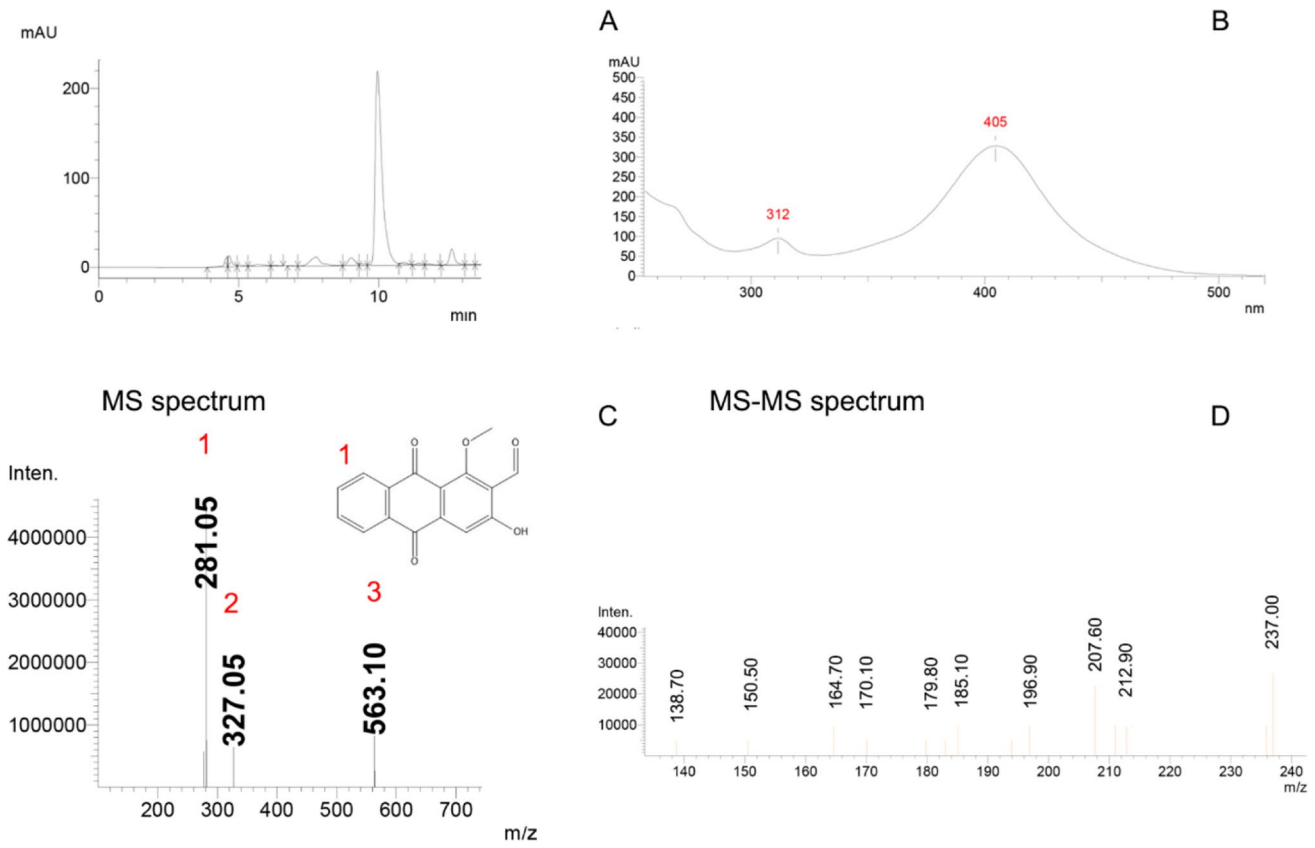

Fig. 5 **A** Chromatogram obtained by UHPLC (t_R = 9.95 min). **B** UV–VIS spectrogram from 200 to 800 nm. **C** Mass and chemical structure spectrum for damnacanthal (numbering detail: 1 = [M-H]$^-$, 2 = [M-H + HCOOH]$^-$, 3 = [M-H + M].$^-$). **D** MS–MS spectrum from *T. australis* sample 2

showed a fluorescence decay less abrupt than the Trolox® standard, with a prolonged effect up to 60 and almost 100 min for *P. murcianum* and *T. australis* samples, respectively, and being comparable to the time of the highest concentration of Trolox®.

Microencapsulation of fungal pigment

Several batches containing microcapsules from *P. murcianum* and *T. australis* pigments were obtained after the process of microencapsulation (Fig. 6). The microcapsules obtained were later characterized through color measurements in CIE *L* a* b** coordinates (Table S1).

Using microscopic tools, the shape, diameter, and diameter distribution of the microcapsules obtained from the selected samples were determined. The shape observed in all the batches produced was normally irregular cubes and spheres (Fig. 7). The size of microcapsules obtained was classified as intermediate, with sizes in the range of 75 and 1000 µm. As per powder characteristics, according to their fineness, the microcapsules were classified as coarse, d_{50} sieve opening = 355–1000 µm. Particle diameter at 10%, 50%, and 90% of the size distribution and particle size dispersal coefficient (Span) are shown in Table 1, where the values of d_{50} for *T. australis* and *P. murcianum* were 329.59 and 543.57 µm, respectively.

Results of the encapsulation efficiency for different batches of fungal microcapsules are shown in Table 2, attaining an average of 40.3% for *T. australis* and 24.9% for *P. murcianum*.

Discussion

The CPC technique was appropriate for fungal pigment separation due to the high retention of the stationary phase, corresponding to the volume of the organic phase of ethyl acetate/n-butanol, which remained inside the equipment upon achieving equilibrium. The total time of this process was approximately 40 min, being faster than the traditional processes of column separation which can take several hours. The great flow rate achieved with the CPC technique can explain this behavior (Friesen et al. 2015).

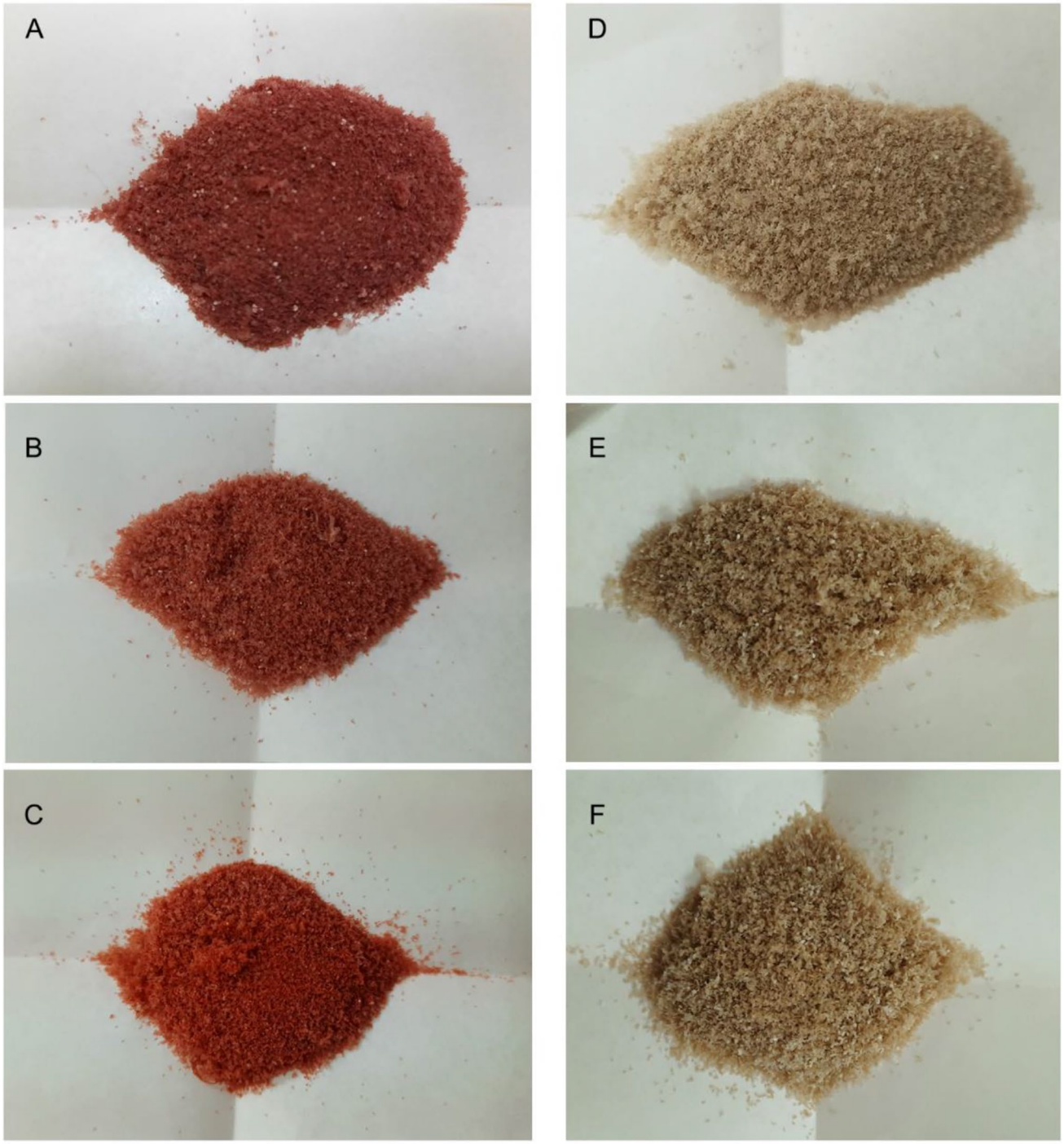

Fig. 6 Microcapsules powder from *T australis* (**A**, **B**, and **C**) and *P. murcianum* (**D**, **E**, and **F**) selected batches

The chemical complexity of the fungal pigments samples was evidenced by the large number of fractions with similar physico-chemical characteristics obtained, which was difficult for the chromatographic separation. Our results strongly suggest the presence of polyketid pigments such as azaphilones and hydroxyanthraquinoids in the fungal extracts. These pigments have demonstrated biological activity which represents an interesting potential for different uses (Frisvad et al. 1990; Visagie et al. 2015).

Measurements in ESI–MS scan mode for *P. murcianum* sample 1 revealed mass values that would correspond to molecular ions of the most abundant pigments of the sample,

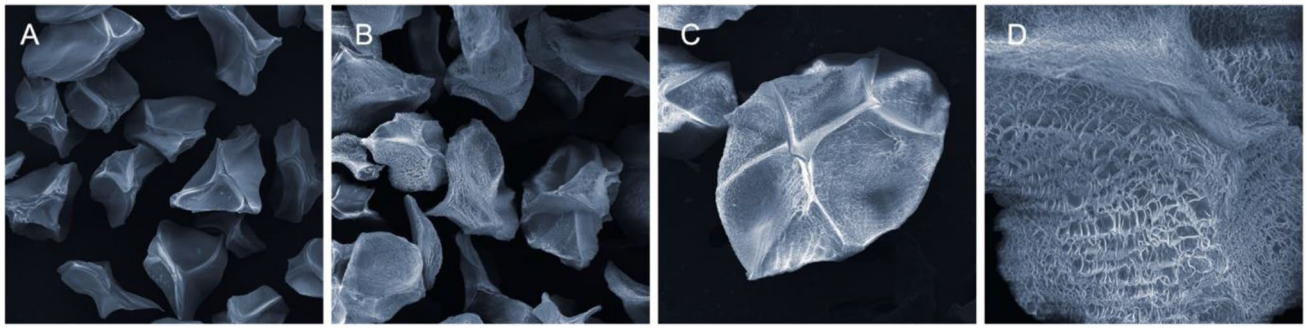

Fig. 7 SEM micrographs showing microcapsules without pigments (226× magnification) (**A**); microcapsules of *P. murcianum* pigments (271×) (**B**); microcapsule of *T. australis* pigments (261×) (**C**); polymeric network in a microcapsule of *P. murcianum* pigments (1550×) (**D**)

Table 1 Particle diameter at 10%, 50%, and 90% of the size distribution and particle size dispersal coefficient (Span) for *T. australis* and *P. murcianum* microcapsules

Sample	Diameter (μm) ± SD			Span
	d_{10}	d_{50}	d_{90}	
Batch C *T. australis*	178.93 ± 0.15	329.59 ± 0.15	480.25 ± 0.15	0.914
Batch E *P. murcianum*	327.33 ± 0.13	543.57 ± 0.13	759.81 ± 0.13	0.796

Table 2 Encapsulation efficiency percentage for *T. australis* and *P. murcianum* microcapsules

Species	Batch	Encapsulation efficiency (%)
T. australis	A	40.4
	B	39.1
	C	41.5
P. murcianum	D	24.4
	E	28.4
	F	22.0

where at least three mass values (*m*/*z*) of 411.15, 421.15, and 438.10 were observed. It is necessary to consider that these values may contain adducts with formic acid (HCOOH) and H_2O due to the high affinity that these pigments would have with the phases used here. When analyzing the molecular weights of known pigments, a mass value of 421.15 was selected. This value is close to the molecular weight of the yellow pigment monascin ($C_{21}H_{26}O_5$, MW = 358.43 g/mol) found in the species of *Monascus* and *Penicillium* (Mapari et al. 2008). In this case, it would be forming an adduct with HCOOH and H_2O, justifying the *m*/*z* value of 421 ($[M\text{-}H + HCOOH + H_2O]^-$). The *m*/*z* value 411 would correspond to the compound monascin without the carbonyl group and forming an adduct with HCOOH and two molecules of H_2O ($[M\text{-}H + HCOOH + 2H_2O\text{-}CO]^-$). Likewise, the *m*/*z* value 438 could correspond to the molecular ion of monascin, forming an adduct with HCOOH and two molecules of H_2O, and with the loss of a second hydrogen $[M\text{-}2H + HCOOH + 2H_2O]^-$. There are some evidences supporting these observations. For instance, according to Mapari et al. (2008), the monascin pigment obtained from the species of *Penicillium* also forms an adduct with acetonitrile and sodium $[M + Na + CH_3CN]^+ = 422.19$, showing absorption peaks at 234, 292, and 394 nm. These data are similar to that obtained in the present study, although in this case the adducts would be formed with HCOOH and H_2O. Another evidence that supports the presence of monascin is reported by Yang et al. (2018), who describe the formation of a product from monascin with a mass value *m*/*z* 331 in ESI (+) for *Monascus* species. This is close to the *m*/*z* 329 obtained in this analysis. Here, a possible adduct with HCOOH and H_2O was detected with a *m*/*z* 411.15 in the mass spectrum. The MS–MS spectrum of the ion 421.15 showed at least six mass values that would correspond to the fragments formed by monascin. All values are theoretically explained, and the possible structures of the fragments are proposed in Figure S2.

UHPLC–DAD–ESI–MS scan mode measurements for *P. murcianum* sample 2 revealed a spectrum that provide a mass value of 319.10, corresponding to the main molecular ion in the fraction. Therefore, the molecular weight should be approx. 320, the value matching with the yellow monashexenone polyketide ($C_{19}H_{28}O_4$, MW = 320.41 g/mol) found in the species of *Monascus* (Patakova 2013; Yuliana et al. 2017). In the MS–MS spectrum of the main molecular ion, it was 319.10, and at least 14 mass values were obtained. These can be explained through the theoretical fragmentation of the chemical structure of monashexenone, described in Figure S3.

UHPLC–MS scan mode measurements for *T. australis* sample 1 showed a spectrum with a mass value of 548.20, which would correspond to the main molecular ion in the pigment, atrorosin H ($C_{29}H_{31}N_3O_8$, MW = 549.55 g/mol).

This pigment has been described as atrorosins (Isbrandt et al. 2019), a new subgroup of *Monascus*-type pigments produced by the species *T. atroroseus* (Tolborg et al. 2020). These pigments are characterized by having an amino acid integrated into the pyridine ring that is part of the base ring of nitrogenated azaphilones, which in this case corresponds to histidine (Isbrandt et al. 2019). The value $[M\text{-}H]^- = 548.20$ is close to that described by Tolborg et al. (2020), who obtain a value of $[M+H]^+ = 550.22$ during LC–MS analysis. The two values could correspond to the molecular weight 549.20, only differing in the type of ionization used (negative and positive, respectively). When analyzing the fragments obtained in the MS–MS spectrum, it was observed that for $[M\text{-}H]^- = 548.20$, at least 9 mass values were produced. These can be explained by the fragmentation of atrorosin H, detailed in Figure S4.

The ESI–MS scan mode revealed for *T. australis* sample 2 a mass spectrum with the *m/z* value of 281.05, corresponding to the main molecular ion in pigment fraction. This signal may correspond to the natural yellow pigment hydroxyanthraquinoid damnacanthal ($C_{16}H_{10}O_5$, MW = 282.25 g/mol) (Caro et al. 2012). The *m/z* of 327.05 observed could be associated to two joined damnacanthal molecules, one of them without a proton ($[M\text{-}H+M]^-$). When analyzing the fragments obtained in the MS–MS spectrum, it was observed that for the *m/z* value of 281.05, 14 mass values were produced, which could correspond to the damnacanthal molecular fragments described in Figure S5.

The chemical characterization of the main pigments that are present in extracellular cultures of the filamentous fungi *P. murcianum* and *T. australis* fractioned by CPC is here described for the first time. In both fungal species, pigments of azaphilone and anthraquinoid class predominated. In the extracts of *P. murcianum*, it was possible to identify compounds responsible for the yellow coloration, such as monascin and monashexenone. In the case of *T. australis*, it was possible to identify the compound responsible for the red coloration, such as atrorosin H, and compounds responsible for the yellow coloration such as damnacanthal. The compounds found here have not been previously described in these fungal species; however, for *T. australis*, other azaphilone-type pigments have been reported (Visagie et al. 2015). Additional spectroscopic analysis such as C-NMR and H-NMR could be performed in the future for definitive confirmation of proposed compounds.

The analysis of the biological activity of the *P. murcianum* and *T. australis* pigments revealed a high antioxidant activity as determined by the ORAC assay. The ORAC values obtained were comparable with those reported by Jin and Pyo (2017). In order to relate the chemical nature of the molecules with the antioxidant effect, several fungal fractions were analyzed in more detail. The Trolox® reagent is a water-soluble synthetic analog of vitamin E, which acts exclusively by reducing the phenolic hydroxyl in the chroman ring (Forrest et al. 1994). The fungal pigments analyzed here could act in similar form, but also act by means of other mechanisms such as free radical scavenging, being substrate for radicals and/or chelation of metal ions. The antioxidant activity in the azaphilones is mainly related with two different mechanisms: direct reaction between radicals and hydroxyl groups linked to aromatic rings, and transformation of molecules in pyridines (Chen et al. 2020). The 4-pyridone and its tautomer, the pyridin-4-ol, are characterized as powerful antioxidants, due to the reactivity of vinyl groups. Although the mechanism is not yet fully clarified, the structure–activity relationship of pyridines derived from azaphilones has been demonstrated (Gao et al. 2013; Ezquerra-Brauer and Chan-Higuera 2021).

The high antioxidant activity (2130 µmol TE/g) detected in sample 1 of *P. murcianum* could be related with some of the mechanisms mentioned above, while being mainly attributed to the presence of monascin pigments. In the case of *T. australis*, the antioxidant effect could be mainly related to anthraquinoid pigments, since sample 2 presented the highest ORAC value (706 µmol TE/g) and contained damnacanthal, which has a proven antioxidant activity (Saha et al. 2013; Li et al. 2017). These results suggest that the great diversity of molecules present in the fungal extracts may act in combined ways presenting a synergistic effect in some cases, or interfering each other in other cases (antagonistic effect). The latter would explain the notable difference in ORAC values of purified fractions versus raw extracts of the fungi. The high antioxidant activity detected in the purified fungal fractions by ORAC assay suggests the potential of these natural pigments as innovative functional ingredients to be used in the cosmetic industry.

The use of microencapsulation allowed the obtention of homogeneous powders containing fungal pigments, which could be useful for the cosmetic industry. In the microcapsules, sharp edges and dotted surfaces with small indentations were observed in some cases (Fig. 6). This may be due to the collapse of the polymeric structure during the lyophilization process. As an automated process, microencapsulation is a fast and simple method to obtain microcapsules of low size distribution. These characteristics are necessary in standardized product, since uniform microcapsules ensure a uniform pigment amount (Swarbrick 2006). The polymeric materials, sodium alginate, hyaluronic acid, and chitosan, used in the process are all biodegradable and bio-compatible, allowing also their application as a sustainable product (Necas et al. 2008; Lupo et al. 2012; Leong et al. 2016; Shariatinia 2019). Optical microscopy contributed to the routine monitoring of the experiments carried out to obtain microencapsulates. On the other hand, scanning microscopy allowed a more detailed analysis of the shape and structure of selected samples.

Another characteristic to be noted is the already reported low toxicity of the extracellular pigments produced by *T. australis* and *P. murcianum*. Cytotoxicity tests conducted by Hernández et al. (2019) provided evidence on the safe nature of these pigments against mammalian cell lines (HEK293 and NIH/3T3) to which pigments and pigment-leachates were applied. In this sense, more research including toxicity test oriented to cosmetic uses, such as immunological test to determine skin hypersensitivity and testing on other skin cell lines, would be appropriate and highly advisable for these fungal pigments.

The results obtained in this work contribute to the chemical and biological characterization of new natural ingredients of fungal origin as an alternative to synthetic ingredients and dyes for industrial use, such as in the cosmetics industry.

Supplementary information The online version contains supplementary material available at https://doi.org/10.1007/s00253-022-12255-9.

Acknowledgements MAB thanks the support of FONDECYT project N° 1171857 and FONDEQUIP project N° 130209. VHC thanks the support of PAI Convocatoria Nacional Subvención a Instalación en la Academia 2018, 77180054 and Fondecyt 11180030. We appreciate the valuable contributions of the reviewers of the first version of this manuscript.

Author contribution PCM: conceptualization, resources, methodology, software, formal analysis, writing—original, writing—review and editing draft, visualization, project administration. MAL: methodology, resources, supervision. EPN: methodology, resources, software, validation, formal analysis, visualization, supervision, writing—review and editing draft. AMH: conceptualization, resources, writing—original draft, writing—review and editing draft. MAB: methodology, software, validation, supervision, writing—review and editing draft. VHC: conceptualization, resources, review and editing draft. MFE: methodology, conceptualization, resources, writing—review and editing draft.

Data availability The datasets generated during and/or analyzed during the current study are available from the corresponding author on reasonable request.

Declarations

Ethical approval This article does not contain any studies with human participants or animals performed by any of the authors.

Conflict of interest The authors declare no competing interests.

References

Aizpurua-Olaizola O, Navarro P, Vallejo A, Olivares M, Etxebarria N, Usobiaga A (2016) Microencapsulation and storage stability of polyphenols from *Vitis vinifera* grape wastes. Food Chem 190:614–621. https://doi.org/10.1016/j.foodchem.2015.05.117

Athamneh T, Amin A, Benke E, Ambrus R, Leopold C, Gurikov P, Smirnova I (2019) Alginate and hybrid alginate-hyaluronic acid aerogel microspheres as potential carrier for pulmonary drug delivery. J Supercrit Fluids 150:49–55. https://doi.org/10.1016/j.supflu.2019.04.013

Aulton M (2002) Pharmaceutics, the science of dosage form design (2nd edn). Churchill Livingstone. https://doi.org/10.1360/zd-2013-43-6-1064

BÜCHI Labortechnik AG (2016) Encapsulator operating manual B-390. https://static1.buchi.com/sites/default/files/downloads/11593481_B-390_OM_es_C_LR_0.pdf?93abfae7b3d811629f5a166c0e4206feafbab924

Caro Y, Anamale L, Fouillaud M, Laurent P, Petit T, Dufosse L (2012) Natural hydroxyanthraquinoid pigments as potent food grade colorants : an overview. Nat Prod Bioprospect 2:174–193

Caro Y, Venkatachalam M, Lebeau J, Fouillaud M, Dufosse L (2015) Pigments and colorants from filamentous. In: Merillon JM, Ramawat K (eds) Fungal Metabolites. Series in Phytochemistry. Springer, Cham. https://doi.org/10.1007/978-3-319-19456-1_26-1

Chaudhary V, Katyal P, Poonia A, Kaur J, Puniya PH (2022) Natural pigment from Monascus: the production and therapeutic significance. J Appl Microbiol 133(1):18–38. https://doi.org/10.1111/jam.15308

Chemat F, Vian M, Cravotto G (2012) Green extraction of natural products: concept and principles. Int J Mol Sci 13(7):8615–8627

Chen C, Tao H, Chen W, Yang B, Zhou X, Luo X, Liu Y (2020) Recent advances in the chemistry and biology of azaphilones. RSC Adv 10(17):10197–10220. https://doi.org/10.1039/d0ra00894j

Combes R, Haveland-Smith R (1982) A review of the genotoxicity of food, drug and cosmetic colours and other azo, triphenylmethane and xanthene dyes. Mutat Res-Rev Genet 98:101–243

Convention TUSP (2007a) (811) Finura de polvos. In USP 30 Farmacopea de los Estados Unidos de América: Formulario Nacional, vol. 2, p 389

Convention TUSP (2007b) Pruebas Físicas (776) Microscopía óptica. In USP 30 Farmacopea de los Estados Unidos de América: Formulario Nacional, p 342

Crebelli R, Conti L, Carere A, Zito R (1981) Mutagenicity of commercial p-phenylenediamine and of an oxidation mixture of p-phenylenediamine and resorcinol in *Salmonella typhimurium* TA98. Food Cosmet Toxicol 19:79–84

Ezquerra-Brauer J, Chan-Higuera J (2021) Antioxidant capacity and mechanism of action of pigments in marine organisms. Biotecnol Cien Agropecuarias 15(2):186–197. https://doi.org/10.29059/cienciauat.v15i2.1501

Feng Y, Shao Y, Chen F (2012) *Monascus* pigments. Appl Microbiol Biot 96:1421–1440. https://doi.org/10.1007/s00253-012-4504-3

Forrest V, Kang Y, Mcclain D, Robinson D, Ramakrishnan N (1994) Oxidative stress-induced apoptosis prevented by trolox. Free Radical Bio Med 16(6):675–684

Friesen J, McAlpine J, Chen S, Pauli G (2015) Countercurrent separation of natural products: an update. J Nat Prod 78:1765–1796

Frisvad J, Samson R, Stolk A (1990) Disposition of recently described species of *Penicillium*. Mol Phylogenet Evol 14(2):209–232

Galindo, E, Peña, C, Serrano-Carreón, L (2008) Domesticar microorganismos en un biorreactor: Los retos del bioingeniero. Una ventana al quehacer científico. Instituto de Biotecnología, Universidad Autónoma de México, pp 131–144. https://bit.ly/3vwqkoY

Gao J, Yang S, Qin J (2013) Azaphilonoids: chemistry and biology. Chem Rev 113(7):4755–4811

Gmoser R, Ferreira J, Lennartsson P, Taherzadeh M (2017) Filamentous *ascomycetes* fungi as a source of natural pigments. Fungal Biol Biotechnol 4(4):1–25

Hernández V, Galleguillos F, Thibaut R, Müller A (2018a) Fungal dyes for textile applications : testing of industrial conditions for wool

fabrics dyeing. J Text Inst 110(1):61–66. https://doi.org/10.1080/00405000.2018.1460037
Hernández V, Galleguillos F, Sagredo N, Machuca Á (2018b) A note on the dyeing of wool fabrics using natural dyes extracted from rotten wood-inhabiting fungi. Coatings 8(77):1–6
Hernández V, Machuca Á, Saavedra I, Chavez D, Astuya A, Barriga C (2019) *Talaromyces australis* and *Penicillium murcianum* pigment production in optimized liquid cultures and evaluation of their cytotoxicity in textile applications. World J Microb Biot 35(10):1–9
Hernández V, Galleguillos F, Sagredo N, Machuca Á (2020) Color fastness of fabrics after dyeing with fungal dyes. Int J Cloth Sci Tech. https://doi.org/10.1108/IJCST-12-2019-0196
Inoue K, Ito Y, Hattori Y, Tsutsumiuchi K, Ito S, Hino T, Oka I (2010) Efficient purification of xanthomonasin A and B high-speed countercurrent from *Monascus* yellow colorant by chromatography. JJFCS 17(3):185–191
Isbrandt T, Tolborg G, Ødum A, Workman M, Larsen T (2019) Atrorosins : a new subgroup of *Monascus* pigments from *Talaromyces atroroseus*. Appl Microbiol Biotechnol 104(2):615–622. https://doi.org/10.1007/s00253-019-10216-3BIOTECHNOLOGICAL
Jin Y, Pyo Y (2017) Effect of *Monascus*-fermented soybean extracts on antioxidant and skin aging-related enzymes inhibitory activities. Prev Nutr Food Sci 22(4):376–380
Jurić S, Jurić M, Król Ż, Vlahoviček K, Vinceković M, Dragović-Uzelac, V, Donsì F (2020) Sources, stability, encapsulation and application of natural pigments in foods. Food Rev Int 38(8):1735–1790. https://doi.org/10.1080/87559129.2020.1837862
Leong J, Lam W, Ho K, Voo W, Lee M, Lim H, Lim S, Tey B, Poncelet D, Chan E (2016) Advances in fabricating spherical alginate hydrogels with controlled particle designs by ionotropic gelation as encapsulation systems. Particuology 24:44–60. https://doi.org/10.1016/j.partic.2015.09.004
Li C, Lin F, Sun W, Yuan S, Zhou Z, Wu F, Chen Z (2018) Constitutive hyperproduction of sorbicillinoids in *Trichoderma reesei* ZC121. Biotechnol Biofuels 11:1–16
Li H, Li X, Li X, Wang C, Liu H, Kassack M, Meng L, Wang B (2017) Antioxidant hydroanthraquinones from the marine algal-derived endophytic fungus *Talaromyces islandicus* EN-501. J Nat Prod 80(1):162–168
Lupo B, González C, Maestro A (2012) Microencapsulación con alginato en alimentos. Técnicas y aplicaciones. RVCTA 3(1):130–151
Mapari S, Meyer A, Thrane U (2006) Colorimetric characterization for comparative analysis of fungal pigments and natural food colorants. J. Agric. Food Chem 54(19):7027–7035. https://doi.org/10.1021/jf062094n
Mapari S, Hansen M, Meyer A, Thrane U (2008) Computerized screening for novel producers of *Monascus*-like food pigments in *Penicillium* species. J Agric Food Chem 56(1):9981–9989
Montenegro A, Nahmad Y, Sarocchi D, Bartali R, Rodríguez L (2011) Optical granulometry by digital image processing. Proc SPIE Int Soc Opt Engs. https://doi.org/10.1117/12.902633
Morales L, Ruiz J, Oliveira J, Sousa M, Méndez A, Giuffrida D, Dufossé L & Montañez J (2020) Biotechnological approaches for the production of natural colorants by *Talaromyces*/*Penicillium*: a review. Biotechnol Adv. https://doi.org/10.1016/j.biotechadv.2020.107601
Necas J, Bartosikova L, Brauner P, Kolar J (2008) Hyaluronic acid (hyaluronan): a review. Vet Med 53(8):397–411. https://doi.org/10.17221/1930-VETMED
Ohta N, Robertson A (2005) Colorimetry: Fundamentals and Applications, 1st edn. John Wiley & Sons, Hoboken
Ou B, Chang T, Huang D, Prior R (2013) Determination of total antioxidant capacity by oxygen radical absorbance capacity (ORAC) using fluorescein as the fluorescence. J Aoac Int 96(6):1372–1377
Patakova P (2013) Monascus secondary metabolites : production and biological activity. J Ind Microbiol Biotechnol 40:169–181
Patil R, Patil M, Maheshwari V (2016) Bioactive secondary metabolites from endophytic fungi : a review of biotechnological production and their potential applications. In Stud Nat Prod Chem 49(1):189–205
Pimenta L, Gomes D, Cardoso P, Takahashi J (2021) Recent findings in azaphilone pigments. J Fungi 7(541):1–29. https://doi.org/10.3390/jof7070541
Pitt J, Hocking (2022) Penicillium and Talaromyces. In Fungi and food spoilage, 4th edn. Springer, p 231–349. https://doi.org/10.1007/978-0-387-92207-2
Poorniammal R, Prabhu S, Dufossé L, Kannan J (2021) Safety evaluation of fungal pigments for food applications. J Fungi 7(692):1–15. https://doi.org/10.3390/jof7090692
Saha K, Lam K, Abas F, Hamzah A, Stanslas J, Hui L, Lajis N (2013) Synthesis of damnacanthal, a naturally occurring 9, 10- anthraquinone and its analogues, and its biological evaluation against five cancer cell lines. Med Chem Res 22(1):2093–2104
Sajid S, Akbar N (2018) Applications of fungal pigments in biotechnology. PAB 7(3):922–930
Shariatinia Z (2019) Pharmaceutical applications of chitosan. Adv Colloid Interface Sci 263:131–194. https://doi.org/10.1016/j.cis.2018.11.008
Shi Y, Pan T (2012) Red mold, diabetes, and oxidative stress : a review. Appl Microbiol Biot 94:47–55
Swarbrick J (2006) Microencapsulation: methods and industrial applications, 2nd edn. Taylor & Francis, Oxford
Tolborg G, Ødum A, Isbrandt T, Larsen T, Workman M (2020) Unique processes yielding pure azaphilones in *Talaromyces atroroseus*. Appl Microbiol Biot 104(2):603–613
Visagie M, Yilmaz N, Frisvad J, Houbraken J, Seifert K, Samson R, Jacobs K (2015) Five new Talaromyces species with ampulliform-like phialides and globose rough walled conidia resembling T. verruculosus. Mycoscience 56(5):486–502. https://doi.org/10.1016/j.myc.2015.02.005
Xiao X, Chu L, Chen W, Zhu J (2005) Monodispersed thermoresponsive hydrogel microspheres with a volume phase transition driven by hydrogen bonding. Polymer 46:3199–3209. https://doi.org/10.1016/j.polymer.2005.01.075
Yan H, Mengzhu Z, Xiaoying D, Dan Z, Han C, Xincai X (2015) Preparation and characterization of alginate-hyaluronic acid-chitosan composite gel beads. J. Wuhan Univ Technol Mater Sci Ed 30(6):1297–1303
Yang H, Li J, Wang Y, Gan C (2018) Identification of water-soluble *Monascus* yellow pigments using HPLC-PAD-ELSD, hight-resolution ESI-MS, and MS-MS. Food Chem 245(1):536–541. https://doi.org/10.1016/j.foodchem.2017.10.121
Ying H, Jiang H, Liu H, Chen F, Du Q (2014) Ethyl acetate-n-butanol gradient solvent system for high-speed countercurrent chromatography to screen bioactive substances in okra. J Chromatogr A 1359:117–123. https://doi.org/10.1016/j.chroma.2014.07.029
Yuliana A, Singgih M, Julianti E, Blanc P (2017) Derivates of azaphilone *Monascus* pigments. Biocatal Agric Biotechnol 9:183–194

Authors and Affiliations

Paulina I. Contreras-Machuca[1,2] · Marcia Avello[1] · Edgar Pastene[3] · Ángela Machuca[4] · Mario Aranda[5] · Vicente Hernández[6,7] · Marcos Fernández[2]

Marcia Avello
maavello@udec.cl

Edgar Pastene
edgar.pastene@gmail.com

Mario Aranda
mario.aranda@uc.cl

Vicente Hernández
vhernandezc@udec.cl

Marcos Fernández
marferna@udec.cl

[1] Pharmacognosy Laboratory, Department of Pharmacy, Faculty of Pharmacy, Universidad de Concepción, Concepción, Chile

[2] Pharmaceutical Technology Laboratory, Department of Pharmacy, Universidad de Concepción, Concepción, Chile

[3] Laboratory of Synthesis and Biotransformation of Natural Products, Universidad del Bio Bio, Chillán, Chile

[4] Fungal Biotechnology Laboratory, Department of Plant Sciences and Technology, Universidad de Concepción, Campus Los Angeles, Los Angeles, Chile

[5] Food and Drug Research Laboratory, Department of Pharmacy, Faculty of Chemistry and Pharmacy, Pontificia Universidad Católica de Chile, Santiago, Chile

[6] Faculty of Forestry, Universidad de Concepción, Concepción, Chile

[7] Biotechnology Center, Universidad de Concepción, Concepción, Chile

Terms and Conditions

Springer Nature journal content, brought to you courtesy of Springer Nature Customer Service Center GmbH (“Springer Nature”).
Springer Nature supports a reasonable amount of sharing of research papers by authors, subscribers and authorised users (“Users”), for small-scale personal, non-commercial use provided that all copyright, trade and service marks and other proprietary notices are maintained. By accessing, sharing, receiving or otherwise using the Springer Nature journal content you agree to these terms of use (“Terms”). For these purposes, Springer Nature considers academic use (by researchers and students) to be non-commercial.
These Terms are supplementary and will apply in addition to any applicable website terms and conditions, a relevant site licence or a personal subscription. These Terms will prevail over any conflict or ambiguity with regards to the relevant terms, a site licence or a personal subscription (to the extent of the conflict or ambiguity only). For Creative Commons-licensed articles, the terms of the Creative Commons license used will apply.
We collect and use personal data to provide access to the Springer Nature journal content. We may also use these personal data internally within ResearchGate and Springer Nature and as agreed share it, in an anonymised way, for purposes of tracking, analysis and reporting. We will not otherwise disclose your personal data outside the ResearchGate or the Springer Nature group of companies unless we have your permission as detailed in the Privacy Policy.
While Users may use the Springer Nature journal content for small scale, personal non-commercial use, it is important to note that Users may not:

1. use such content for the purpose of providing other users with access on a regular or large scale basis or as a means to circumvent access control;
2. use such content where to do so would be considered a criminal or statutory offence in any jurisdiction, or gives rise to civil liability, or is otherwise unlawful;
3. falsely or misleadingly imply or suggest endorsement, approval , sponsorship, or association unless explicitly agreed to by Springer Nature in writing;
4. use bots or other automated methods to access the content or redirect messages
5. override any security feature or exclusionary protocol; or
6. share the content in order to create substitute for Springer Nature products or services or a systematic database of Springer Nature journal content.

In line with the restriction against commercial use, Springer Nature does not permit the creation of a product or service that creates revenue, royalties, rent or income from our content or its inclusion as part of a paid for service or for other commercial gain. Springer Nature journal content cannot be used for inter-library loans and librarians may not upload Springer Nature journal content on a large scale into their, or any other, institutional repository.
These terms of use are reviewed regularly and may be amended at any time. Springer Nature is not obligated to publish any information or content on this website and may remove it or features or functionality at our sole discretion, at any time with or without notice. Springer Nature may revoke this licence to you at any time and remove access to any copies of the Springer Nature journal content which have been saved.
To the fullest extent permitted by law, Springer Nature makes no warranties, representations or guarantees to Users, either express or implied with respect to the Springer nature journal content and all parties disclaim and waive any implied warranties or warranties imposed by law, including merchantability or fitness for any particular purpose.
Please note that these rights do not automatically extend to content, data or other material published by Springer Nature that may be licensed from third parties.
If you would like to use or distribute our Springer Nature journal content to a wider audience or on a regular basis or in any other manner not expressly permitted by these Terms, please contact Springer Nature at

onlineservice@springernature.com